ELSEVIER

Sensors and Actuators A 71 (1998) 198–207

SENSORS AND ACTUATORS A PHYSICAL

A new hybrid technology for planar microtransformer fabrication

O. Dezuari, S.E. Gilbert, E. Belloy, M.A.M. Gijs *

Institute of Microsystems, Swiss Federal Institute of Technology (EPFL), CH-1015 Lausanne, Switzerland

Received 18 March 1998; accepted 21 May 1998

Abstract

We have developed a new printed circuit board (PCB) technology adapted for the fabrication of ultra-flat microtransformers. The two outer layers of the PCB stack comprise the electrical windings of the inductive devices, while the inner layer is made of a micro-patterned amorphous magnetic ribbon with extremely high relative magnetic permeability ($\mu_r \approx 100000$). Two basic configurations were considered; one being based on a toroidal magnetic core and the other on a rectangular (E-shaped) magnetic core. The electrical properties of the microtransformers have been studied as a function of frequency. Inductances were found to be as much as 30 μH at 1 kHz, a relatively high value compared to microtransformers of similar size. Despite a relatively high leakage flux, voltage transformation efficiencies were measured between 89% and 98%. The high performance of these devices is primarily due to the use of the high permeability magnetic core. The characteristics of these devices are discussed in light of geometrical considerations and finite element calculations.

Keywords: Planar transformers; PCB technology; High permeability material; Vitrovac®

1. Introduction

There is a large interest today in the realization of miniaturized inductive devices for signal transformation, sensitive magnetic field detection or switch-mode power supply applications. Often these devices determine, to an important extent, the size of the complete application in which they are employed. Therefore, we have developed microfabrication techniques for the realization of small and flat inductive devices with still appreciable inductive values.

In the recent literature, several examples of micromachined transformers have been reported. Park et al. [1] reported on 0.5 cm size inductors based on a 15 μm thick electroplated $Ni_{80}Fe_{20}$ and $Ni_{50}Fe_{50}$ magnetic cores. The structure is realized by a number of sputter deposition, electroplating, photoresist spinning and patterning steps. Inductance values of 0.5 μH were reported at 10 kHz.

Löchel et al. [2] have used thick resist technology, sputtering and clever electroplating/etching methods to fabricate coils of a few mm size, based on NiFe core material. Inductance values of order of 1 μH were reported at 125 kHz. This work and the previous one are primarily demonstrations of new micromachining technology, and an application such as power inductors or transformers was not considered. Thus, all measurements were done at small primary excitation voltages so that eddy current and magnetic hysteresis losses would be minimized.

Microtransformers of 5 mm size integrated with diodes on a Si wafer were also reported by Mino et al. [3,4]. These transformers with transformation ratio of 1 are based on an amorphous magnetic core prepared by sputtering, in the form of 3 separate layers of CoZrRe, each 5 μm thick, with 0.1 μm SiO_2 spacer layers. This layered configuration was chosen exactly to reduce eddy current losses in the magnetic core. Reported inductance values were in the range of 0.5–1 μH.

A specially configured transformer of about 4 cm size was realized by Yamasawa et al. [5] by sandwiching primary and secondary coils in between two 10 μm thick amorphous CoZr layers. An inductance value of 5 μH and a power throughput of around 1 W was obtained by this rather large device of 40×30 mm.

It may be clear that for an appreciable inductance value within a rather small volume, it is very important to have a core material within the inductor or transformer that has a very high relative magnetic permeability μ_r. Today, magnetic alloys with extremely high μ_r values can be fabricated by splash-cooling the molten alloy into an amorphous state. One type of such material, which is commercially available, is the Vitrovac® family of magnetic alloys. For this work, a partic-

* Corresponding author. Tel.: +41-21-693-6734; Fax: +41-21-693-6670; E-mail: martin.gijs@epfl.ch

0924-4247/98/$ - see front matter
PII S0924-4247(98)00185-X

ular alloy, known under the trade name Vitrovac® 6025, (composition $(Co,Fe,Mo)_{73}(Si,B)_{27}$), was chosen primarily because of its extremely high relative permeability ($\mu_r \approx 100{,}000$) [7]. This material is already employed as core material for three-dimensional magnetic amplifier chokes, where the transition from a high inductance at low fields to a low inductance at saturation is used in a high speed on/off switch for power converter applications [8].

This paper describes the fabrication and characterization of flat microtransformers of two basic geometries. The inductive devices are composed of three layers of which the outer layers carry the printed coil patterns and the inner layer is the Vitrovac® 6025 high permeability ferromagnetic sheet core. Both magnetic metal and copper layers are patterned using standard lithographic techniques. In between the magnetic metal and copper layers there is a foil of solid epoxy glue (typically 100 μm) for insulation and assembly. Such material is well known in the assembly of multilayer PCB structures. Connection between the outer copper patterns is realized by electroplating methods to complete the windings. These transformers are about 600 μm thick, with lateral dimensions approximately 1 cm and inductance values in the 10 μH range.

2. Choice of the magnetic core

As mentioned earlier, Vitrovac® 6025 was chosen because of its very high permeability, thus allowing inductive devices composed of this material to possess relatively high inductances. In addition to the high μ_r, the material is characterized by a low coercive field H_c (typically 0.003 A/m), and a saturation field Bs of 0.55 T. Vitrovac® ribbon (25 μm thick) is also very flexible, yet has a high tensile and shear strength, rendering it highly suitable for the fabrication of thin layer devices, both rigid and flexible. The interested reader is referred to the manufacturer's literature for more details [7,8].

3. Transformer design

Two different types of transformers have been designed and fabricated: the first type has the inner magnetic foil patterned into a toroidal shape and the second type has a magnetic core of rectangular shape (E-core). Diagrams of these two structures are displayed in Fig. 1. An example of a toroidal transformer, characterized by an outer radius A and inner radius B for the toroidal-shaped Vitrovac, is shown in Fig. 1a. We have kept A constant at 6.9 mm, while B took on values of either 3.9 or 5.3 mm.

One should note that in Fig. 1a, the primary windings are divided into two groups, which have been symmetrically positioned at both sides of the secondary windings. A typical ratio for the number of turns between the primary and secondary windings N_{prim}/N_{sec} is 18/5. However, it is possible

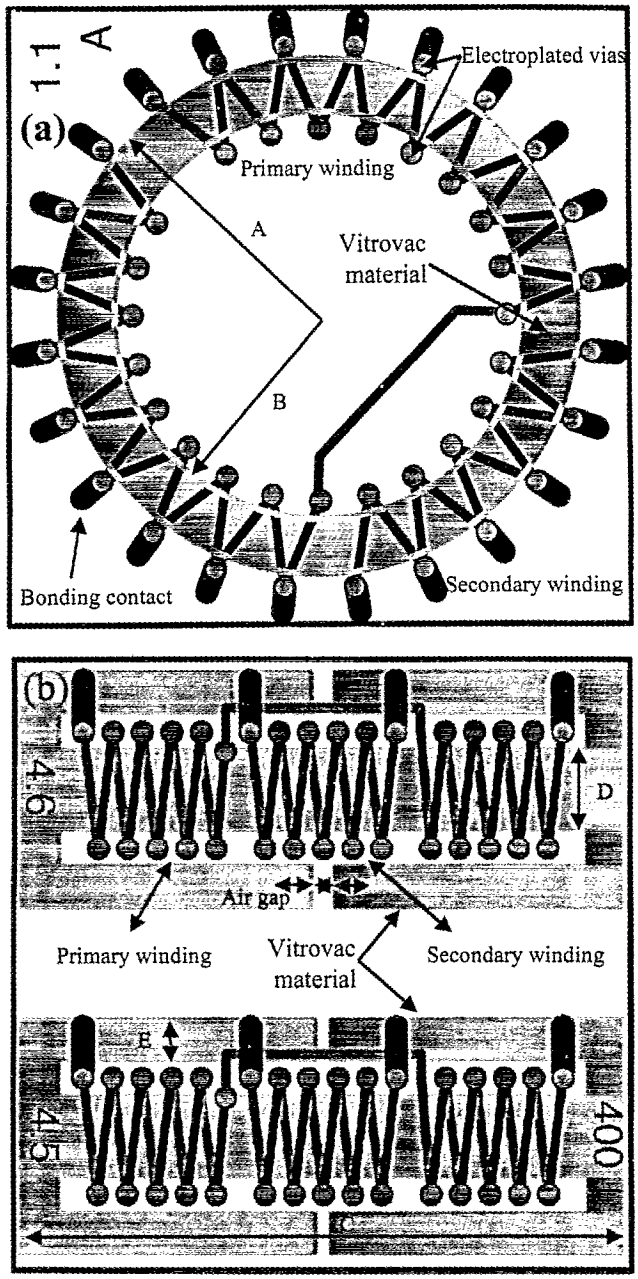

Fig. 1. Schematic diagram of (a) a toroidal, and (b) two rectangular μ-transformers.

to characterize the transformer for a number of windings N_{prim} between 1 and 18, as bonding pads have been incorporated for each winding.

Fig. 1b shows two rectangular E-core transformer whose primary windings have been grouped into two clusters of five, and are symmetrically positioned around the five secondary windings. All windings are around the inner magnetic part of the structure, while flux closure of the magnetic circuit is obtained via the two outer 'legs' of the magnetic core. Dimensions for this type of transformer are $C = 16$ mm, $D = 2$ mm and $E = 1$ mm. Moreover, we have introduced air gaps in the outer two legs of the magnetic material. A series of E-core transformers with gap widths varying between 0 and

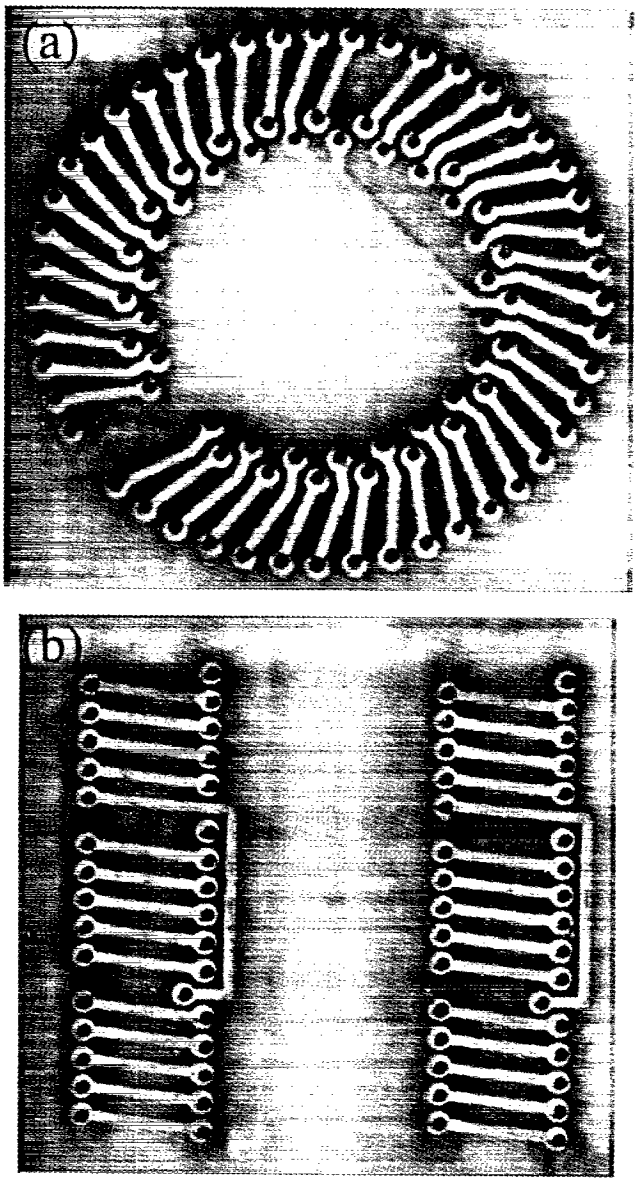

Fig. 2. Photographs of as-fabricated transformers: (a) a toroidal microtransformer; (b) two rectangular microtransformers showing air gaps.

1000 μm were fabricated to investigate how the inductance of such transformer behaves as a function of the width of the gap, as will be discussed below. Photographs of the experimental realization of the two types of transformers are displayed in Fig. 2.

4. Fabrication process

A schematic diagram of the coil fabrication process is shown in Fig. 3. The proposed device fabrication is very similar to a conventional PCB process. These devices are based on two epoxy boards (100 μm thick) with copper (35 μm thick) laminated on one side, and by a simple epoxy board (100 μm thick) as support for the Vitrovac® magnetic foil. A liquid epoxy was used to laminate the magnetic foil

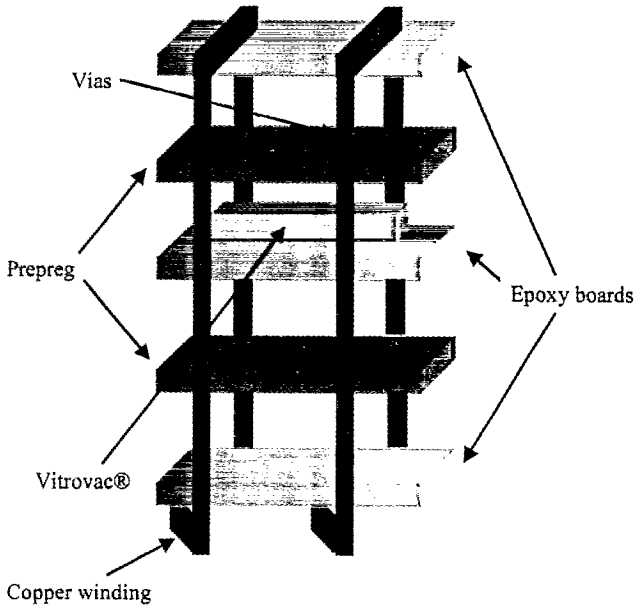

Fig. 3. Schematic diagram of coil fabrication process.

on the inner epoxy board. Two 100 μm-thick sheets of prepreg solid epoxy were used for bonding the laminates into a stack of five layers.

The Vitrovac® 6025 foil was patterned photolithographically to form the transformer cores by first laminating sheets of solid negative photoresist (Ordyl® 200 [9]) onto degreased foils, and then processing according to manufacturer's specifications after pattern transfer. A wet chemical process was developed in-house to etch the magnetic foils, consisting of exposure of the resist-covered foils to a freshly prepared aqua regia type etching bath (HNO_3:HCl:H_2O, 2:1:3) for several minutes at room temperature without agitation. The photoresist proved itself immune to the etchant, and exhibited excellent adhesion if the substrates were well cleaned.

To align the layers, a pinning system was used. The precision of the alignment holes define the maximum lateral precision available with this technology (currently about 100 μm). Bonding operations were carried out by hot pressing typically at 180°C and 20 kg/cm^2. During the bonding step, the epoxy sheets melt, whereby the viscous liquid spreads out and contacts all interior surfaces under the applied pressure.

Via holes were drilled at appropriate positions for the interconnects, which were subsequently metallized using copper electroplating. Winding patterns were produced on the outer copper layers photolithographically, thereby completing the helical coil pattern which fully encircles the interior core.

5. Measurements

The transformers have been electrically characterised using an HP4194A Impedance/Gain-Phase analyzer. Inductance and resistance values are recorded simultaneously as a function of a logarithmic frequency sweep from 100 Hz up to 20 MHz, using sinusoidal excitation signal levels of 100

and 500 mV rms. Transformers are measured from the primary side with the secondary windings both open and shorted, and from the secondary side with both the primary open and shorted. By doing these four measurements for each transformer, it is possible to provide an equivalent circuit with a well determined main and leakage inductance, as will be discussed below. Measurements of gain were made to determine actual transformation ratios. For these measurements, the transformers were configured with a 50 Ω load across the secondary, using an input signal level of 0 dBm (1 mW).

6. Results

6.1. Main inductance and resistance

Typical frequency response characteristics of the primary main inductance, $L_{m,p}$, of toroidal transformers are shown in Fig. 4, for different number of windings N. These curves were obtained with an open secondary. The monotonic decrease of $L_{m,p}$ with frequency is in part due to the intrinsic behavior of the magnetic material, which exhibits a similar dependence [8]. Fig. 4 clearly shows that $L_{m,p}$ increases with increasing N, an effect predicted to follow a parabolic power law (N^2) for an ideal inductor. The power law dependence of the toroidal and rectangular transformers is shown in Fig. 5a,b, respectively. The deviations from N^2 behavior at low winding number (and hence, low intrinsic $L_{m,p}$) may be due to spurious lead inductance and capacitive effects.

Primary winding resistances R_P have been plotted in a similar fashion in Fig. 6. For each curve, R_P remains constant at lower frequencies, then begins to rise. The onset point of this resistance increase occurs at progressively lower frequencies as N increases. Dissipative core losses in the form of magnetization hysteresis and eddy currents are responsible for the augmentation of R_P. Indeed, at larger N, hence larger magnetic flux, these losses become more important.

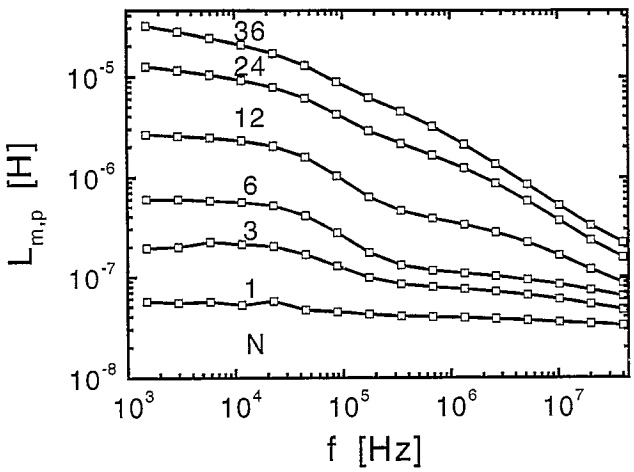

Fig. 4. Inductance vs. frequency for toroidal microtransformers with varying number of turns. Inner radius B of the magnetic material is 5.3 mm.

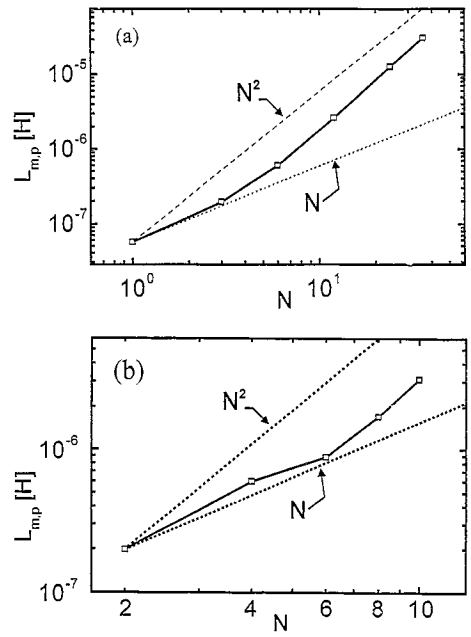

Fig. 5. Power-law dependence of primary inductance L on number of windings N for (a) toroidal, and (b) rectangular transformers.

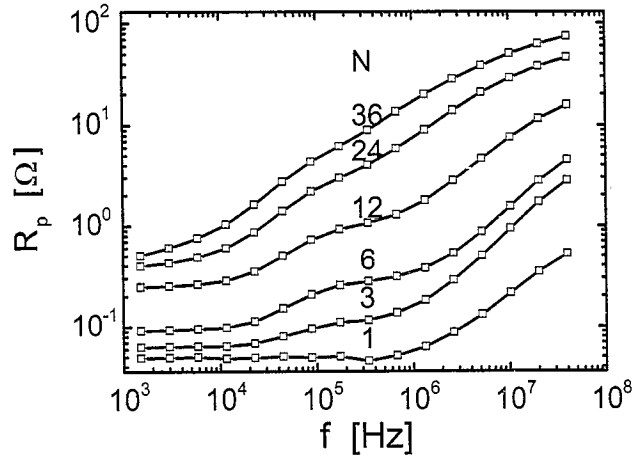

Fig. 6. Resistance vs. frequency for toroidal microtransformers with varying number of turns. Inner radius B of the magnetic material is 5.3 mm.

6.2. Measurements of leakage inductance

Not all flux generated by the primary of the transformer may be coupled into the secondary windings, but rather can be closed via a path in the air. This quantity of 'lost' flux is characterized by the leakage inductance, L_l, and its magnitude is partly related to the spacing, or pitch, between coil windings. In order to elucidate the influence of the winding pitch on the leakage flux, we present in Fig. 7 finite element simulations of the distribution of induced magnetic flux adjacent to the coil, using maxwell (Ansoft) 3D finite element software. In the ideal case, where the windings are in intimate contact, as shown in Fig. 7a, the flux lines emanating from the windings are seen to circulate around the whole coil. In this case, all the flux generated by the individual windings is fully

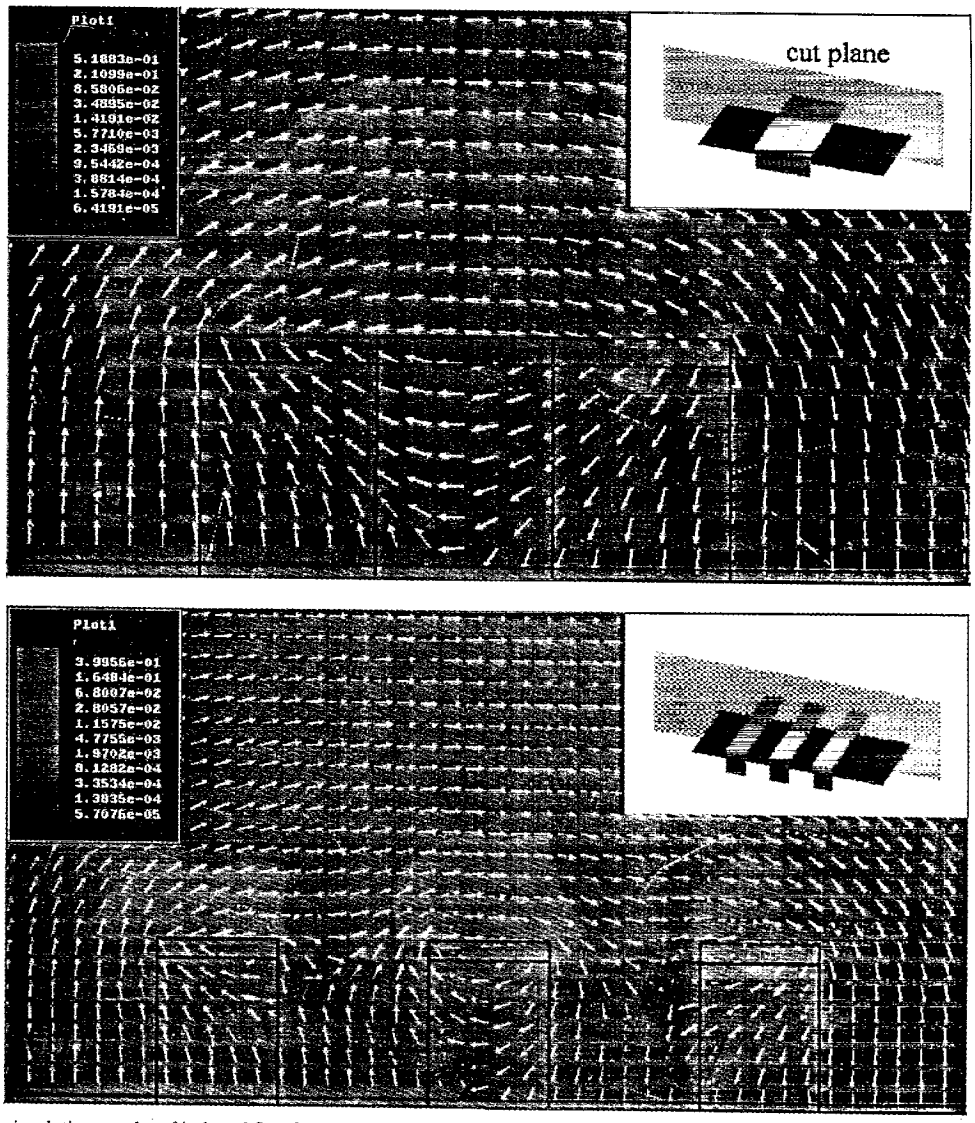

Fig. 7. Finite element simulation results of induced flux field around a model coil composed of three windings, demonstrating the influence of the winding pitch on the leakage flux. (a) zero winding pitch; (b) a winding pitch of 250 μm.

coupled to form a global, or main flux for the entire coil. The results of a similar simulation based on a model coil with a winding pitch of 250 μm is shown in Fig. 7b. It is seen in this figure that a significant portion of the generated flux does not couple to the core, and tends to localize itself in the immediate vicinity of the individual windings. This uncoupled flux, which does not participate in the main flux of the coil is part of the leakage flux. Generally, for a transformer, all flux generated by the primary windings, which 'leaks away' in the air and is not coupled into the magnetic material positioned within the secondary windings, represents a leakage inductance.

One method of measuring the leakage inductance respectively for both the primary ($L_{l,p}$) and secondary ($L_{l,s}$) coils by measuring the inductance while the opposite coil of the transformer is short-circuited [10,11]. The measured inductance is then the leakage inductance, as this inductance, and its associated flux, is not compensated by currents induced in the opposite coil. It is important that the leakage inductance be minimized to improve transformation efficiency, but it also can be critically important in high frequency operation in order to protect semiconductor components in switching converter circuits [10].

In Fig. 8, we show plots of the primary main ($L_{m,p}$) and leakage ($L_{(l,p)}$) inductances for both toroidal and rectangular transformers. At low frequencies, the two inductance curves tend to merge because of the very low reactance of the self inductances at these frequencies ($\approx$0.01–0.2 Ω at 1 kHz), compared to the winding DC resistances ($\approx$0.1–0.5 Ω). Thus at low frequencies, the secondary does not really 'see' a zero ohm load, thus obscuring the leakage inductance measurement. However at higher frequencies (10^4–10^5 Hz), the coil reactances are much greater relative to the coil DC resistances, and indeed the inductances are seen in Fig. 8 to be well separated, thus permitting a reasonable estimation of the leakage inductance.

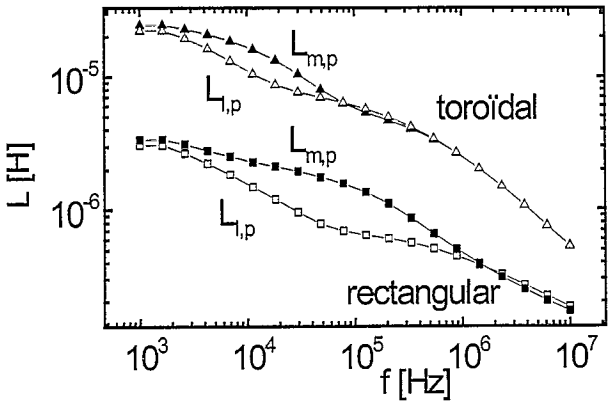

Fig. 8. Toroidal microtransformer main and leakage inductances (filled and open triangles, respectively). Same for a rectangular microtransformer (filled and open squares, respectively).

We represent these inductances in a series equivalent circuit [10–12] shown in Fig. 9, wherein any stray capacitances that may exist have been ignored, as they have been too small to detect experimentally. The electrical relationship between the leakage inductance L_l and the main inductance L_m is revealed in this schematic. The resistive element $R_{loss,l}$ represents the coil resistance of the windings plus the dissipative core losses engendered by the leakage inductance L_l. $R_{loss,m}$ represents the core losses engendered by the main inductance L_m, and R'_{load} is the load resistance connected across the secondary (and transformed back to the primary). All resistive elements that characterize the primary coil are combined with their secondary coil counterparts which are referred to the primary (value multiplied by the factor N_{prim}/N_{sec}), so that the transformer can be represented entirely by the primary circuit. If R'_{load} is infinite, as in the case of an open secondary, the current in the primary is forced to flow through both L_l and L_m. If it is zero, as in the case of a shorted secondary, then L_m and $R_{loss,m}$ are shunted, and L_l is the only inductance remaining in the circuit. Hence, in the frequency intervals of 10^4–10^5 Hz in Fig. 8, the curves with open symbols represent L_l, and those with closed symbols represent $L_l + L_m$. The data sets are shown for the primaries of both types of transformers, but measurements for the secondaries are very similar. Typical values of L_m and L_l, derived from the curves in Fig. 8, and $R_{loss,l} + R_{loss,m}$, derived from curves in Fig. 6, for toroidal and rectangular transformers are listed in Tables 1 and 2, respectively, at selected frequencies. In general, the leakage inductance, as determined by this method of measure, is between 40%–50% of the total inductance 5–30 kHz frequency range for the toroidal, and the 50–130 kHz range for the rectangular microtransformers. One way to minimize this relatively high value for L_l is by reducing the winding pitch, which in the present case is as large as 250 μm. Yamada et al. [6] have shown by simulation that the leakage flux, to which the leakage inductance is proportional, in microtransformers of a design similar to ours, already can approach 10% of the total flux with a winding pitch of only 25 μm.

Table 1
Values for main and leakage inductance, plus combined main and leakage and core loss resistances at selected frequencies for a toroidal microtransformer

Frequency (Hz)	$L_m + L_l$ (H)	L_m (H)	L_l (H)	$R_{loss,l} + R_{loss,m}$ (Ω)
5 880	1.92×10^{-5}	1.10×10^{-5}	8.20×10^{-6}	0.71
11 590	1.56×10^{-5}	7.94×10^{-6}	7.60×10^{-6}	0.90
28 840	1.19×10^{-5}	6.21×10^{-6}	5.2×10^{-6}	1.15

Table 2
Values for main and leakage inductance, plus combined main and leakage core loss resistances at selected frequencies for a rectangular microtransformer without gap

Frequency (Hz)	$L_m + L_l$ (H)	L_m (H)	L_l (H)	$R_{loss,l} + R_{loss,m}$ (Ω)
48 330	1.76×10^{-6}	9.80×10^{-7}	7.80×10^{-7}	0.34
74 480	1.56×10^{-6}	8.71×10^{-7}	6.89×10^{-7}	0.47
127 400	1.34×10^{-6}	6.98×10^{-7}	6.42×10^{-7}	0.69

6.3. Influence of air gaps

The effect of introducing air gaps in the outer legs of rectangular E-core type transformers is demonstrated in Fig.

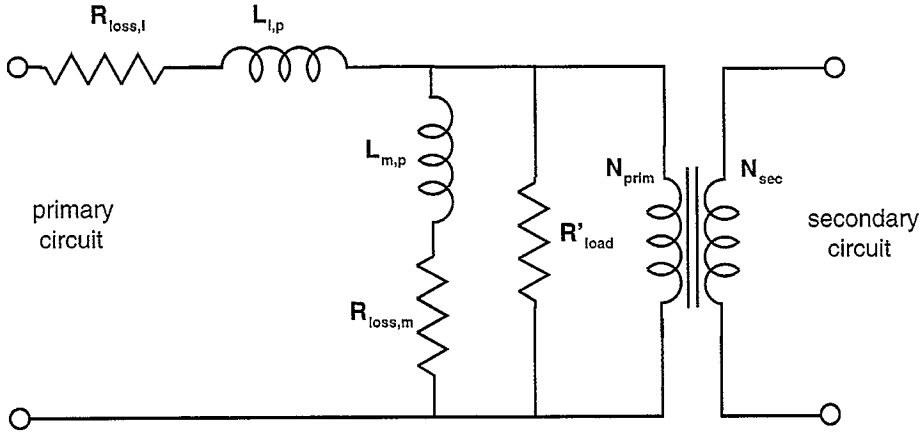

Fig. 9. Simplified equivalent circuit of a transformer. See text for explanation of symbols.

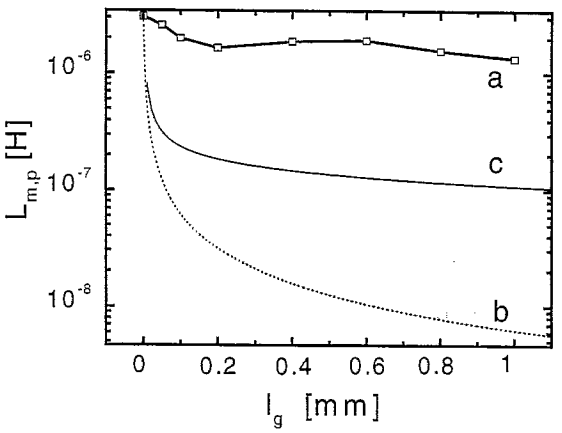

Fig. 10. Primary main inductance vs. air gap at 1 kHz for transformers with rectangular magnetic core and $N=10$: (a) measured value; (b) calculated value without fringe correction factor (c) calculated value including fringe correction.

10 (curve a). The inductance $L_{m,p}$ falls as the gap increases, thus behaving in a manner analogous to that of conventional transformers. However, $L_{m,p}$ maintains a rather constant value after the gap reaches 200 μm. To a first approximation, the dependence of $L_{m,p}$ on gap width l_g is given by:

$$L_{m,p}=\mu_0 N^2 A_c/(l_g+l_m/\mu_r) \quad (1)$$

where μ_0 is the permeability of free space, A_c is the cross-sectional area of the inner core leg, and l_m is the path length in the magnetic material. The other symbols have their usual meanings. This equation is plotted as curve b in Fig. 10, based on an effective μ_r of 16 000, and l_m of 33.1 mm. However, the experimental values are grossly underestimated by this theoretical curve, which predicts a more rapid fall-off of $L_{m,p}$ than is observed. Flux fringing around the gap, an effect which becomes more evident as the gap grows larger, can decrease the overall reluctance of the magnetic circuit, thereby offsetting the effect of the increasing gap. This effect is not taken into account by Eq. (1). A finite element calculation of the magnetic induction around a rectangular microtransformer with a large gap is shown in Fig. 11. This simulation qualitatively demonstrates how the fringing flux is distributed around the gap. Its effect can also be estimated quantitatively by introducing a multiplicative correction factor, F, into Eq. (1), where $F=1+l_g/A_c^{1/2}\ln(2G/l_g)$ [10,11]. G is the vertical dimension of the core window ($G=14$ mm in our case).

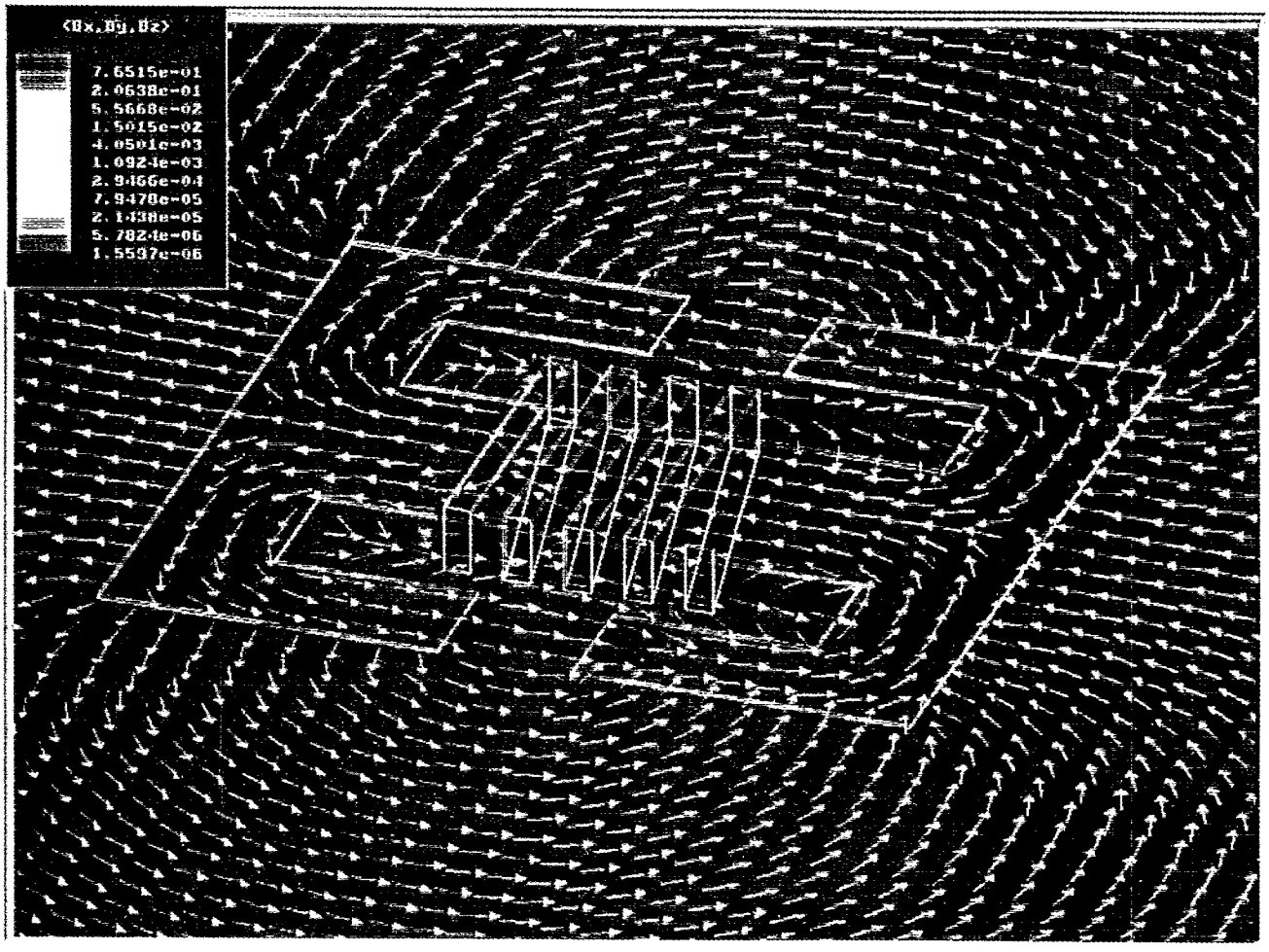

Fig. 11. Finite element simulation of flux field distribution around a rectangular microtransformer with a gap of 1 mm. The simulated field shows the formation of fringing flux around the gaps.

We have plotted Eq. (1) with the correction as curve (c) in Fig. 10, demonstrating that there is better agreement with the experimental data. Thus, fringing flux at least partially accounts for the observed behavior, but a secondary effect, that being the closure of the flux lines across the window space from the outer to the inner core legs as the gap width becomes very large (1 mm), may also play a significant role. This effect, which would be more important in microtransformers than in conventional ones, would reduce the mean length of the magnetic circuit l_m. This point remains to be clarified, however.

6.4. Transformer gain measurements

Fig. 12a,b are typical gain (V_{sec}/V_{prim}) plots for toroidal and rectangular microtransformers, the latter with and without gap. The gain plots are measures of the real voltage transformation ratios, and are indicative of the microtransformers' performance over a wide frequency range. In Fig. 12a, the gain for a toroidal transformer in step-down configuration is plotted. This graph reveals that it has a flat response of −12 dB starting at about 20 kHz and extending to about 1 MHz. This decibel level corresponds to a voltage ratio of 0.25. Taking into account the turns ration of 18:5, ideally one would expect a voltage transformation ratio of 0.28. Thus, the measurement shows that this microtransformer has a 89% voltage transformation efficiency over almost two decades of frequency in the step-down configuration.

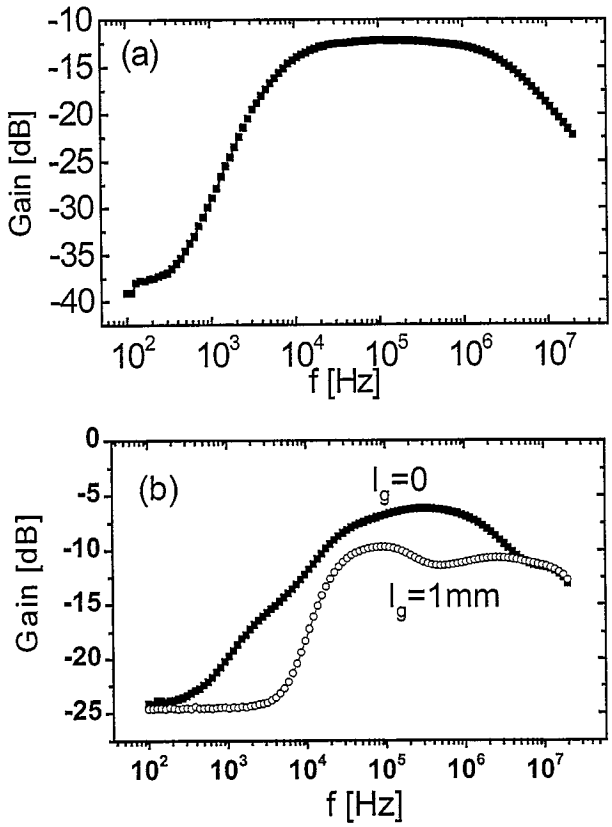

Fig. 12. Frequency dependence of transformation gain (a) for a toroidal microtransfomer, and (b) for rectangular microtransformers without gap (filled squares) and with air gap width $l_g = 1$ mm (open circles).

Transformation gain curves are shown for rectangular microtransformers (with and without gap) in Fig. 12b. For a rectangular transformer without a gap in a step-down configuration with a 2:1 turns ratio, the efficiency is slightly higher than that of the torus, as the gain peaks at −6.2 dB at approximately 300 kHz, corresponding to a voltage transformation ratio of 0.49, or a 98% efficiency. The gain rests above −7 dB (89% efficiency) for frequencies ranging between 78 kHz to 1 MHz (see Fig. 11a, upper curve). The gain curve for a rectangular transformer with a 1 mm gap is distinguished by a sharp rise starting at about 5 kHz, with a maximum of −9.7 dB at 113 kHz (Fig. 11b, lower curve), corresponding to a voltage transformation ratio of 0.33, or 66% transformation efficiency. Beyond this point, the gain is fairly flat over a very wide frequency range, and stays above −11 dB (56% efficiency) at all frequencies between 30 kHz to over 6 MHz. The lower transformer gain can be explained by a relatively larger importance of flux leaking away in the air.

7. Discussion

The remarkably high permeability of Vitrovac® foil as the magnetic core is the key factor in achieving a relatively high inductance in a small planar configuration. Toroidal core microtransformers reported in this work typically exhibited primary winding inductances above 7 μH at frequencies below 100 kHz, with maximal inductances of about 30 μH at 1 kHz, and approximately 2 μH at 1 MHz. This compares with typical inductance values well below 1 μH for other types of planar microtransformer configurations with similar dimensions [1–4,13]. Both the toroidal and rectangular microtransformers exhibit relatively high leakage inductances (over 40%) as measured by a standard technique. Further optimization of the coil design and placement, in the form of reduction of winding pitch and closer proximities of the primary and secondary, would allow reductions in the leakage flux, as explained above. Nevertheless, both types of microtransformers in a step-down configuration were characterized by fairly flat gain responses at frequencies spanning 2 to 3 decades. A flat gain response corresponding to transformation efficiencies of 89% across a frequency range of about 20 kHz to about 1 MHz, for the torus, and greater than 89% between 78 kHz to 1 MHz, with a peak of 98% at 500 kHz for the rectangular configuration, were measured.

The introduction of an air gap in the magnetic core generally greatly reduces inductance, and hence the effective permeability, by increasing the reluctance, of the magnetic circuit, as expected. As demonstrated in this work, however, flux closure across the core window can be more important than the fringing flux in offsetting the influence of the gap as its width approaches that of the window. Efforts are underway to further understand this effect, and will be elaborated upon in a future publication. The presence of the air gap also lowers

the efficiency of the microtransformer, and in the specific case detailed above, the voltage transformation efficiency was reduced to 66% from a peak value of 98% when a gap of 1 mm was introduced in the magnetic core.

8. Conclusions

The data presented in this paper demonstrate that the proposed hybrid technology is capable of producing planar microtransfomer with performance characteristics that are equal to and even surpass those of previously reported devices of similar size. For the latter, more costly thin film fabrication techniques were employed in their fabrication. The frequency range for maximum efficiency has been shown to span a range of 20 kHz to 1 MHz, an order of magnitude lower than the optimal operation range for other planar microtransformers of similar size [1–5,13], which generally need to be operated in the MHz range to compensate the reduction in size.

This new hybrid PCB/magnetic metal foil technology permits the facile development of high inductance planar components. In comparison with existing planar inductor technologies, this new process virtually eliminates the need for time consuming and expensive thin film deposition techniques, while retaining compatibility with standard electronic packaging schemes. The use of industrially compatible processes based on inexpensive epoxy board substrate permits the reduction of costs and facilitates mass production at later stages. The cost aspects, mass production capabilities, and high degree of flexibility offered by the choice of different magnetic materials are reasons to propose this new hybrid technology as a serious alternative to the currently available micromachined magnetic devices.

Acknowledgements

The authors would like to thank Mr Marc Hermanjat and Mr Philippe Vossler of the Department of Electrical Engineering at EPFL for their assistance in the process conception, and Mr Pavel Kejik of the Institute of Microsystems for his help with the simulation program.

References

[1] J.Y. Park, L.K. Lagorce, M.G. Allen, Ferrite-based integrated planar inductors and transformers fabricated at low-temperature, IEEE Trans. Magn. 33 (1997) 3322–3324.
[2] B. Löchel, A. Maciossek, M. Rothe, W. Windbracke, Microcoils fabricated by UV depth lithography and galvanoplating, Sensors and Actuators A 54 (1996) 663–668.
[3] M. Mino, T. Yachi, A. Tago, K. Yanagisawa, K. Sakakibara, A new planar microtransformer for use in micro-switching converters, IEEE Trans. Magn. 28 (1992) 1969–1973.
[4] M. Mino, T. Yachi, A. Tago, K. Yanagisawa, K. Sakakibara, Planar microtransformer with monolithically integrated rectifier diodes for micro-switching converters, IEEE Trans. Magn. 32 (1996) 291–296.
[5] K. Yamasawa, K. Maruyama, I. Hirohama, P.P. Biringer, High frequency operation of a planar-type microtransformer and its application to multilayered switching regulators, IEEE Trans. Magn. 26 (1990) 1204–1209.
[6] N. Yamada, Y. Yokoyama, H. Tanaka, Fabrication of wrapped micro coils wound around a magnetic core, Transducers'95 -Eurosensors IX, 1995, 272–275.
[7] Vitrovac® product literature, Vacuumschmeltze, Hanau, Germany 1996.
[8] R. Boll, Weichmagnetische Werkstoffe, Vacuumschmelze, Hanau, Germany, 1990.
[9] Ordyl® AF 200 product literature, Elga Ronal, Milan, Italy.
[10] W.T. McLyman, Transformer and Inductor Design Handbook, 2nd edn., Marcel Dekker, New York, 1988, p. 150.
[11] R. Lee, L. Wilson, C.E. Carter, Electronic Transformers and Circuits, 3rd edn., Wiley, New York, 1988.
[12] W.M. Flanagan, Handbook of Transformer Design and Applications, 2nd edn., McGraw-Hill, New York, 1993.
[13] H. Tsujimoto, T. Koiso, Characteristic in the 0.01 GHz–2.6 GHz range of film transformer with coils on both sides of flexible polyamide film, IEEE Trans. Magn. 32 (1996) 4980–4982.

Biographies

Olivier Dezuari was born in Lausanne, Switzerland, in 1972. He received his diploma in microengineering from the Swiss Federal Institute of Technology, EPF Lausanne in 1997. His diploma project was the simulation, fabrication and characterization of a capacitive microphone for photoacoustic detection. He joined in September 1997 the Institute of Microsystems as research assistant in the field of developing new technologies for the fabrication of inductive components, in particular flexible components.

Scott E. Gilbert received his PhD in physical chemistry from the University of California, Santa Barbara in 1993 after completing a thesis on semiconductor surface electrochemistry. He then came immediately at the Swiss Federal Institute of Technology in Lausanne (EPFL) to postdoc at the Institute of Physical Chemistry for work on nanostructured liquid junction photovoltaic devices. Afterwards, he moved to the Department of Physics where his interests expanded to explore novel methods for ultra-thin metallic film and magnetic nanowire electrodeposition and electrical contacting methods. He is now with Professor Gijs in the Institute of Microsystems as project leader for the development of new technologies for miniature inductive devices and electrochemical micromachining.

Eric Belloy was born in Geneva, Switzerland, in 1972. He received his diploma in microengineering in 1997 from the Swiss Federal Institute of Technology of Lausanne (EPFL). His diploma work was the study, realisation and characterisation of microtips on Si and glass substrates, for the detection of the electrical activity of nerve cells. Since April 1997, he works as research assistant in the Institute of Microsystems at EPFL and is developing a new technology based on flex-foil patterning and assembling, in order to realise magnetic devices.

Martin A.M. Gijs received his degree in physics in 1981 from the Katholieke Universiteit Leuven, Belgium and his PhD degree in physics at the same university in 1986. He joined the Philips Research Laboratories in Eindhoven, Netherlands, in 1987. Subsequently, he has worked there on micro- and nano-fabrication processes of high critical temperature superconducting Josephson and tunnel junctions, the microfabrication of microstructures in magnetic multilayers showing the giant magnetoresistance effect, the design and realisation of miniaturised motors of hard disk applications and the design and realisation of planar transformers for miniaturised power applications. He joined the Swiss Federal Institute of Technology Lausanne (Ecole Polytechnique Fédérale de Lausanne) in 1997 as a professor in the Institute of Microsystems of the Microengineering Department, where he is responsible for the Microsystems Technology group. His main interests are in developing technologies for novel inductive-type devices, new microfabrication technologies for microsystems fabrication in general and the development and use of microsystems technologies for biomedical applications in particular.